Intraperoxisomal redox balance in mammalian cells: oxidative stress and interorganellar cross-talk

Oksana Ivashchenko[a], Paul P. Van Veldhoven[a], Chantal Brees[a], Ye-Shih Ho[b], Stanley R. Terlecky[c], and Marc Fransen[a]

[a]Laboratory of Lipid Biochemistry and Protein Interactions, Department of Molecular Cell Biology, Katholieke Universiteit Leuven, 3000 Leuven, Belgium; [b]Institute of Environmental Health Sciences, Wayne State University, Detroit, MI 48201; [c]Department of Pharmacology, Wayne State University School of Medicine, Detroit, MI 48201

ABSTRACT **Reactive oxygen species (ROS) are at once unsought by-products of metabolism and critical regulators of multiple intracellular signaling cascades. In nonphotosynthetic eukaryotic cells, mitochondria are well-investigated major sites of ROS generation and related signal initiation. Peroxisomes are also capable of ROS generation, but their contribution to cellular oxidation–reduction (redox) balance and signaling events are far less well understood. In this study, we use a redox-sensitive variant of enhanced green fluorescent protein (roGFP2-PTS1) to monitor the state of the peroxisomal matrix in mammalian cells. We show that intraperoxisomal redox status is strongly influenced by environmental growth conditions. Furthermore, disturbances in peroxisomal redox balance, although not necessarily correlated with the age of the organelle, may trigger its degradation. We also demonstrate that the mitochondrial redox balance is perturbed in catalase-deficient cells and upon generation of excess ROS inside peroxisomes. Peroxisomes are found to resist oxidative stress generated elsewhere in the cell but are affected when the burden originates within the organelle. These results suggest a potential broader role for the peroxisome in cellular aging and the initiation of age-related degenerative disease.**

Monitoring Editor
Suresh Subramani
University of California, San Diego

Received: Nov 29, 2010
Revised: Feb 17, 2011
Accepted: Feb 17, 2011

INTRODUCTION

Reactive oxygen species (ROS) are a group of highly reactive oxygen-containing molecules generated as common by-products of normal cellular metabolism (Dowling and Simmons, 2009). Because it is well known that ROS are able to damage all major building blocks of the cell, these molecules are thought to play critical roles in aging, age-related pathologies, and carcinogenesis (Roberts and Sindhu, 2009). However, at controlled levels, ROS also function as intracellular signaling molecules in diverse biological processes such as cell proliferation and differentiation, inflammatory reactions, and immune responses (Fialkow *et al.*, 2007). Cells manage ROS by expressing an array of detoxifying enzymes involved in the maintenance of redox homeostasis (Circu and Aw, 2010). An imbalance between ROS production and elimination alters the cellular redox state and is generally considered a risk factor for the development of various diseases (Salmon *et al.*, 2010).

Currently, it is widely assumed that in nonphotosynthetic eukaryotic cells the majority of ROS is generated by leakage from the mitochondrial electron transport chain (Mammucari and Rizzutto, 2010). However, because peroxisomal respiration may be responsible for as much as 20% of the oxygen consumption of tissues such as liver, and ~35% of all hydrogen peroxide (H_2O_2) formed in rat liver is generated by peroxisomal oxidases (de Duve and Baudhuin, 1966), peroxisomes may also be acting as important mediators of ROS-mediated signaling. The observation that the organelle's ability to maintain the balance of H_2O_2-generating and H_2O_2-degrading activities is compromised in certain disease states as well as during

This article was published online ahead of print in MBoC in Press (http://www.molbiolcell.org/cgi/doi/10.1091/mbc.E10-11-0919) on March 3, 2011.

Address correspondence to: Marc Fransen (marc.fransen@med.kuleuven.be).

Abbreviations used: 3-AT, 3-amino-1,2,4-triazole; DCF, 2′,7′-dichlorofluorescein; DTT, dithiothreitol; EGFP, enhanced green fluorescent protein; GSH, glutathione; GSTK1, glutathione S-transferase kappa 1; H2DCF-DA, dihydrodichlorofluorescein diacetate; HBSS, Hank's balanced salt solution; HuF, human fibroblast; KSKL, prototypic PTS1 targeting signal for peroxisomal matrix proteins; MEF, mouse embryonic fibroblast; MEM, minimum essential medium; PBS, phosphate-buffered saline; PRDX5, peroxiredoxin 5; PTS1, C-terminal targeting signal for peroxisomal matrix proteins; RFI, relative fluorescence intensity; roGFP2, redox-sensitive variant of the enhanced green fluorescent protein; ROS, reactive oxygen species; TMR, tetramethyl rhodamine; WT, wild-type.

aging is certainly in line with this hypothesis (Legakis *et al.*, 2002; Schrader and Fahimi, 2006; Bonekamp *et al.*, 2009).

Peroxisomes contain multiple enzymes that produce H_2O_2, superoxide ($O_2^{\bullet-}$), or nitric oxide (NO) as metabolic by-products (Antonenkov *et al.*, 2010; Van Veldhoven, 2010). In addition, they contain a panel of antioxidant defense enzymes, such as catalase, Cu/Zn-superoxide dismutase (SOD1), and peroxiredoxin 5 (PRDX5) (Antonenkov *et al.*, 2010). The consequences of disequilibrium with respect to these metabolic processes are currently under intense investigation. It has been suggested that peroxisomal abnormalities and aging are linked (Terlecky *et al.*, 2006); however, it is unclear at present the extent to which defects in peroxisomal metabolism lead to cellular and organismal pathologies.

It has been suggested that the mechanism by which nongenotoxic peroxisome proliferators induce hepatocellular carcinomas in rodents is through a sustained increase in the intrahepatic production of ROS as a result of persistent peroxisome proliferation (Reddy *et al.*, 1982; Kasai *et al.*, 1989). However, this idea has been challenged by others claiming the age-dependent effects of rodent hepatocarcinogenic peroxisome proliferators are mediated through abnormalities in cell growth and communication (Suga, 2004).

Human patients suffering from an inherited deficiency of catalase, the most abundant peroxisomal antioxidant enzyme, were reportedly asymptomatic save minor ulcerative oral lesions caused by H_2O_2-containing antiseptics, or H_2O_2-generating bacteria or inflammatory cells (Takahara and Miyamoto, 1948; Takahara, 1952). More recent studies suggest that these individuals face an increased risk of developing age-related diseases including diabetes, atherosclerosis, and cancer (Góth and Eaton, 2000). Mice lacking catalase seem to be healthy for up to 1 yr of age (Ho *et al.*, 2004); what happens later is unclear. Of course, mild phenotypes may be explained by a compensatory activation of antioxidant mechanisms in the knockout background (Antonenkov *et al.*, 2010).

To gain insight into the potential (patho)physiological role of peroxisomes in the aging process and the onset of diseases related to oxidative stress, we monitored the peroxisomal redox state at the single-cell level under basal and stress conditions by employing a redox-sensitive variant of enhanced green fluorescent protein (EGFP) (roGFP2-PTS1). roGFP2 contains engineered cysteine residues (S147C and S204C) and has two fluorescence excitation maxima at ~400 and 490 nm (Hanson *et al.*, 2004). Because oxidation of the dithiol pair causes reciprocal changes in emission intensity when excited at the two different wavelengths, the fluorescence ratios can provide accurate insight into the redox environment of the chromophore (Dooley *et al.*, 2004; Hanson *et al.*, 2004). The use of this ratiometric redox sensor has several advantages over dihydrodichlorofluorescein diacetate (H_2DCF-DA), the "classical" compound used to evaluate cellular oxidative stress (Karlsson *et al.*, 2010). Indeed, as a ratiometric probe, roGFP2 reduces or eliminates distortions of data caused by photobleaching, sensor concentration, variable cell thickness, and nonuniform sensor distribution within cells or between groups of cells (Hanson *et al.*, 2002). In addition, it was recently shown that the oxidation of nonfluorescent H_2DCF-DA to 2′,7′-dichlorofluorescein (DCF) requires the presence of either cytochrome c or both redox-active transition metals and H_2O_2, suggesting the increase in DCF fluorescence may not be a result of exposure to ROS but rather could also reflect the relocation of lysosomal iron and/or mitochondrial cytochrome c to the cytosol (Karlsson *et al.*, 2010). Finally, H_2DCF-DA is oxidized by ROS in an irreversible manner (Meyer and Dick, 2010). To induce oxidative stress in peroxisomes, we used a variant of KillerRed (KillerRed-PTS1); this photosensitizer produces singlet oxygen and superoxide radicals upon green light illumination, even after bleaching (Bulina *et al.*, 2006; Carpentier *et al.*, 2009).

RESULTS

Characterization of roGFP2-PTS1 as a peroxisomal redox indicator

To monitor the redox state of the peroxisomal lumen in single living cells, we constructed a mammalian expression vector designed to append KSKL, a prototypic PTS1 targeting signal for peroxisomal matrix proteins (Lametschwandtner *et al.*, 1998), to the C-terminus of roGFP2 (roGFP2-PTS1). To verify that roGFP2-PTS1 was indeed targeted to the peroxisomal matrix, the construct was expressed in control ($5^{+/+}$ wild-type [WT]) and Pex5p-deficient ($5^{-/-}$) mouse fibroblasts. Pex5p functions as the import receptor for PTS1-containing matrix proteins, and in cells lacking Pex5p, PTS1 matrix protein import is fully impaired (Williams and Stanley, 2010). Our observations that roGFP2-PTS1 colocalized with the peroxisomal membrane protein Pex14p in control cells (Figure 1A) and displayed a diffuse cytosolic staining pattern in $5^{-/-}$ cells (Figure 1B) confirmed that roGFP2-PTS1 is properly targeted to the peroxisomal matrix upon expression in wild-type cells.

Because our goal is to use roGFP2-PTS1 as a probe to monitor redox changes in the peroxisomal matrix in response to altered environmental conditions, we first verified the oxidation state of the reporter protein in cells cultivated under normal conditions and whether it could be further oxidized or reduced. Therefore, we incubated the immortalized mouse embryonic fibroblasts (MEFs) expressing roGFP2-PTS1 for 20 min in phosphate-buffered saline (PBS) containing a membrane-permeant reductant (e.g., dithiothreitol [DTT]) or oxidant (e.g., 4,4-dithiobispyridine [Aldrithiol-4]). A brief exposure of the cells to DTT decreased the 400/480-nm excitation ratio of roGFP2-PTS1, and treating the cells with Aldrithiol-4 resulted in rapid oxidation of the reporter protein (Figure 2, A and B). These observations indicate that roGFP2-PTS1 is a suitable probe to monitor redox changes in the peroxisomal matrix in living cells.

In a proof-of-principle experiment, we investigated whether or not the peroxisomal redox balance could be perturbed by cultivating MEFs in standard growth medium supplemented with cadmium ions (Cd^{2+}), an environmentally relevant sulfhydryl-reactive heavy metal, which has been shown to inhibit cellular antioxidant systems (Henkler *et al.*, 2010). As shown in Figure 2B, this treatment led to a significant increase in the oxidation state of roGFP2-PTS1. In contrast, cultivating cells in the presence of low concentrations of copper (Cu^{2+}) or zinc ions (Zn^{2+}) did not affect the redox state of the peroxisomal matrix (Figure 2B).

Comparison of the redox state of roGFP2 in peroxisomes, mitochondria, and the cytosol

We next compared the oxidation state of roGFP2 in peroxisomes, mitochondria, and the cytosol of immortalized MEFs. Representative fluorescence microscope images of the subcellular distribution pattern of the roGFP2 fusion proteins (roGFP2-PTS1, mt-roGFP2, and c-roGFP2, respectively) are shown in Supplemental Figure S1. Our results indicate that, under the culture conditions used, the redox environment of the peroxisomal matrix is slightly more oxidizing than the cytosol (Figure 3A) but less oxidizing than the redox environment of the mitochondrial matrix (Figure 3B). A statistical analysis of these measurements ($n = 73$) showed that the differences observed were significant ($p < 0.0001$). Note that, because the fluorescence spectra of roGFP2 are known to respond rapidly to pH variations (Hanson *et al.*, 2004) and the in situ pH values for peroxisomes (6.9–8.2; the exact value remains the subject of debate) and

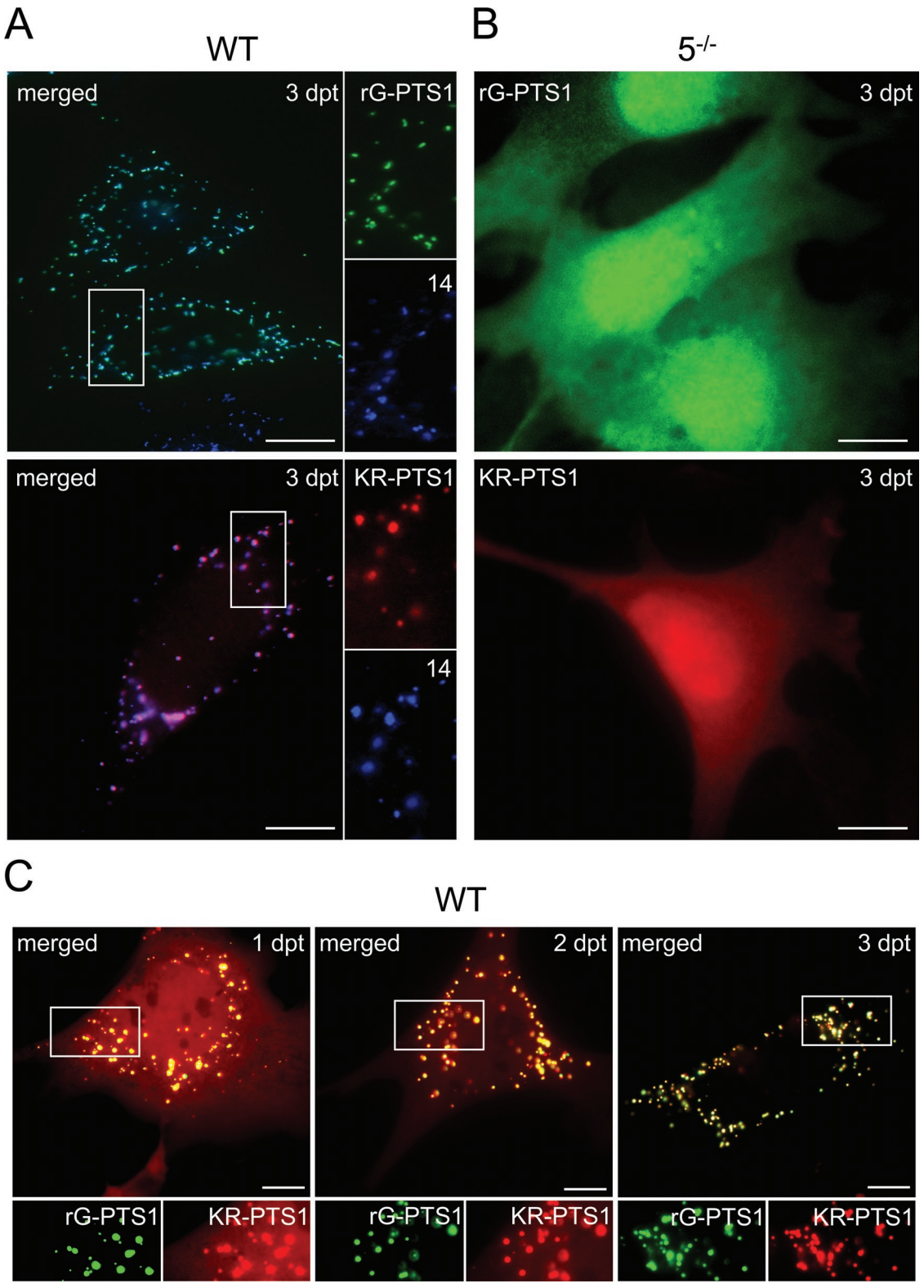

FIGURE 1: Subcellular localization of roGFP2-PTS1 and KillerRed-PTS1. Control (WT) and Pex5p-deficient ($5^{-/-}$) immortalized MEFs were transiently transfected with plasmids encoding roGFP2-PTS1 (green) and/or KillerRed-PTS1 (red). The cells were (B and C) used for live-cell imaging or (A) fixed and processed for immunostaining with an anti-Pex14p (14) antibody, followed by a secondary antibody conjugated to Alexa Fluor 350 (blue). Dpt, day(s) posttransfection; bars, 10 μm.

mitochondria (7.8–8.0) may be slightly different (Casey *et al.*, 2010, and references therein), it could be argued that the differences in redox state between peroxisomes and mitochondria are the result of different pH values inside these organelles. However, this pH-dependent fluorescence quenching affects both the 400- and 480-nm excitation wavelengths of roGFP2 equally, and the calculation of

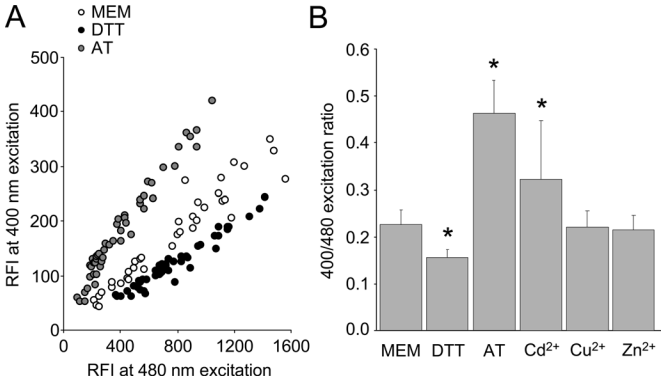

FIGURE 2: RoGFP2-PTS1 is a suitable probe to monitor redox changes in the peroxisomal matrix. Immortalized wild-type MEFs were transiently transfected with a plasmid encoding roGFP2-PTS1 and cultivated in standard growth medium (MEM). After 2 d, the cells were incubated for 1) 20 min in PBS containing 10 mM DTT (DTT) or 10 mM Aldrithiol-4 (AT), or 2) 44 h in MEM supplemented with 10 μM of $CdCl_2$ (Cd^{2+}), $CuCl_2$ (Cu^{2+}), or $ZnCl_2$ (Zn^{2+}). Fluorescence micrographs were taken and analyzed as described in *Materials and Methods*. The relative fluorescence intensities (RFIs) emitted from 400- and 480-nm excitation were (A) plotted against each other or (B) used to calculate the 400/480-nm excitation ratio. The ratio values represent the mean ± SD (n ≥ 50). The data were statistically compared (*p < 0.0001 for DTT, AT, and Cd^{2+} compared with MEM).

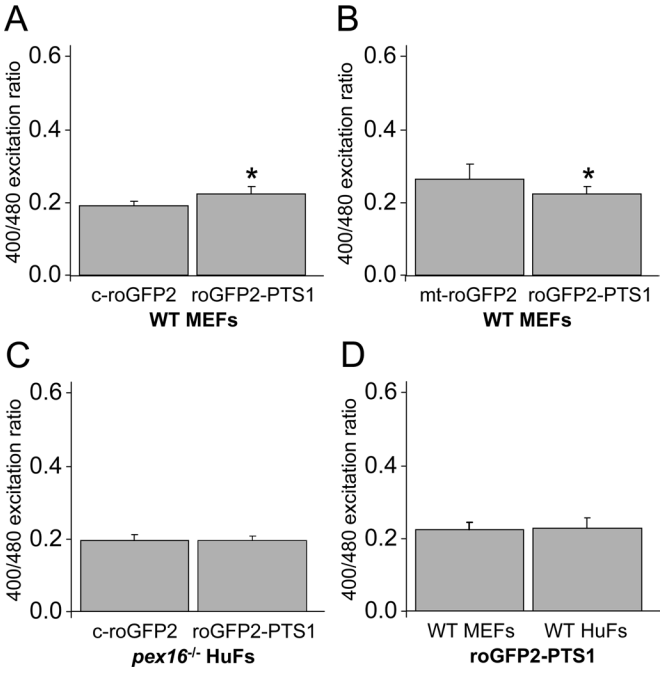

FIGURE 3: In situ measurements of the oxidation state of roGFP2 fusion proteins in mammalian cells. Immortalized mouse embryonic fibroblasts (MEFs) and primary human fibroblasts (HuFs, passage 12) were transiently transfected with a plasmid encoding cytosolic (c-roGFP2), peroxisomal (roGFP2-PTS1), or mitochondrial (mt-roGFP2) roGFP2, and cultivated in standard growth medium. After 2 d, fluorescence micrographs of live cells were obtained and analyzed as described in *Materials and Methods*. (A–D) The RFIs emitted from 400- and 480-nm excitation were used to calculate the 400/480-nm excitation ratio. The ratio values represent the mean ± SD (A and B, n = 75; C and D, n ≥ 50). Each set of data was statistically compared (*p < 0.0001). WT, wild-type cells; *pex16*$^{-/-}$, cells deficient in the peroxin Pex16p.

excitation ratios effectively cancels out any pH effect in the range between 5.5 and 8.0 (Schwarzländer *et al.*, 2008). To exclude the possibility that the small but significant changes in excitation ratio between cytosolic and peroxisomal roGFP2 are an indirect result of the addition of the PTS1 sequence, we also determined the oxidation state of roGFP2 in primary human fibroblasts (HuFs) lacking peroxisomes because of a mutated *PEX16* gene (Honsho *et al.*, 1998) (Figure 3C). No significant difference in the degree of oxidation was found (n ≥ 50). Note that the degree of oxidation of peroxisomally localized roGFP2-PTS1 was virtually identical in immortalized MEFs and primary HuFs (passage number 12) (Figure 3D).

Because the reduction of roGFP2 in vivo is thought to occur through interaction with glutaredoxins (Schwarzländer *et al.*, 2009; Meyer and Dick, 2010), and to date no such proteins have been identified in mammalian peroxisomes, we investigated the ability of roGFP2-PTS1 to recover from oxidative insult. For comparison, we also included analyses of mitochondrial and cytosolic roGFP2. Exposure of cells to 1-mM Aldrithiol-4 elicited immediate and strong oxidative responses (Figure 4, left). Importantly, after moving the cells back to a regular medium, the redox status of all roGFP2 proteins rapidly returned to basal levels (Figure 4, left). Next we investigated whether roGFP2-PTS1, mt-roGFP2, and c-roGFP2 are suitable sensors to visualize redox changes under more physiologically relevant conditions. To accomplish this task, we first subjected the cells to amino acid starvation and subsequently recultivated them in regular medium. Within minutes from the onset of cultivation in starvation medium, the redox state of all roGFP2 proteins decreased (Figure 4, right; statistical analyses revealed significant differences [p < 0.001] for all roGFP2s after 1 h in Hank's balanced salt solution [HBSS]). Again, by recultivating the cells in standard growth medium, the oxidation states of all sensors returned to basal levels (Figure 4, right). Note that the latter treatment resulted in a transient but significant (p < 0.0001) ROS burst in mitochondria and the cytosol. These experiments clearly show that the roGFP2 proteins used in this study can respond quickly, and reversibly, to local changes in the redox state. Our data also indirectly suggest that mammalian peroxisomes contain glutaredoxins or glutaredoxin-like proteins. One such enzyme may be glutathione S-transferase kappa 1 (GSTK1), a protein located within peroxisomes and mitochondria whose physiological function remains to be established (Morel *et al.*, 2004; Antonenkov *et al.*, 2010). Structural studies have demonstrated that GSTK1 proteins not only possess a thioredoxin domain that binds GSH in a similar manner to glutaredoxins but also contain an active site motif that is analogous to that of glutaredoxins (Oakly, 2005).

While this study was in progress, Sakai and coworkers reported the development of a new genetically encoded fluorescence resonance energy transfer probe, Redoxfluor, which can be used to visualize redox states in the cytosol and peroxisomes (Yano *et al.*, 2010). As, to our surprise, these authors reported that the redox state within peroxisomes was more reductive than that in the cytosol, we repeated our roGFP2-PTS1 and c-roGFP2 measurements in cells grown in F-12 nutrient mixture (Yano *et al.*, 2010) instead of minimum essential medium (MEM) alpha medium (see *Materials and Methods* for more details). These experiments showed that the intraperoxisomal but not the cytosolic redox environment is strongly influenced by the culture medium (Figure 5, A and B): the intraperoxisomal redox environment is more oxidizing than the cytosol when the cells are cultured in MEM alpha medium (Figure 5C), and more reducing when the cells are grown in the F-12 nutrient mixture (Figure 5D). Further analysis identified ascorbic acid as the main component responsible for this

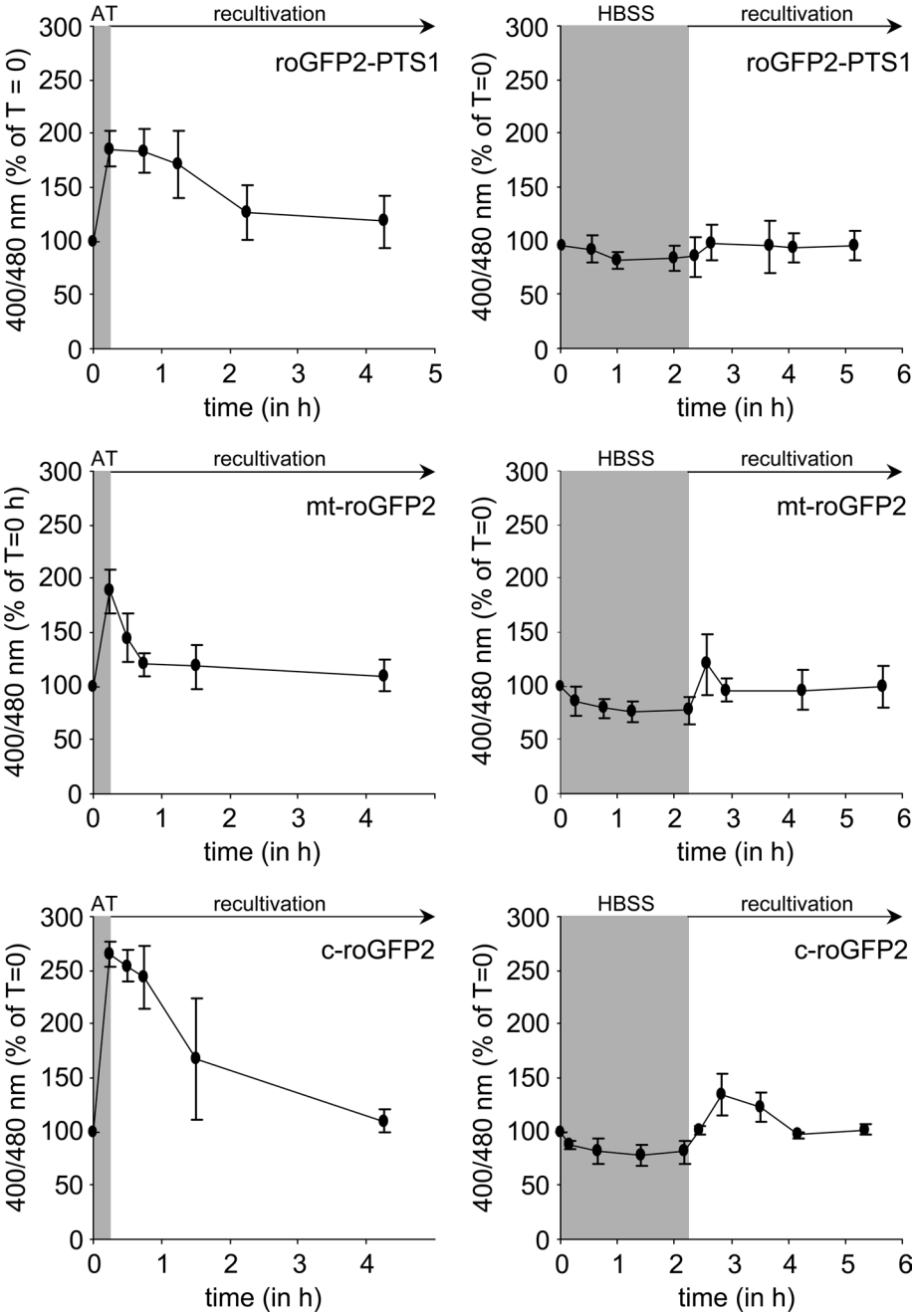

FIGURE 4: Peroxisomal, mitochondrial, and cytosolic roGFP2 respond to exogenous and endogenous oxidative changes. Immortalized wild-type MEFs were transiently transfected with a plasmid encoding cytosolic (c-roGFP2), mitochondrial (mt-roGFP2), or peroxisomal (roGFP2-PTS1) roGFP2 and cultivated in standard growth medium (MEM). After 3 d, the cells were incubated (shaded areas) for 5 min in PBS containing 1 mM of Aldrithiol-4 (AT) or for 130 min in HBSS. Afterward the cells were recultured in MEM. Fluorescence micrographs were taken at the indicated time points and analyzed as described in *Materials and Methods*. The relative fluorescence intensities emitted from 400- and 480-nm excitation were used to calculate the 400/480-nm excitation ratios. The ratios at T = 0 are indicated as 100% ($n \geq 50$).

Intraperoxisomal redox balance and organellar aging

To investigate whether the redox state of the peroxisomal matrix is changing during the aging process of the organelle, we 1) pulse-labeled COS-7 cells expressing HaloTag-catalase (H-cat) with the HaloTag tetramethyl rhodamine (TMR) ligand (Huybrechts *et al.*, 2009; Delille *et al.*, 2010), 2) transfected these cells with the plasmid encoding roGFP2-PTS1 after removal of the ligand, and 3) determined the redox ratio of the biosensor in the pool of preexisting (pulse-labeled) and newly formed (nonlabeled) peroxisomes at different postlabeling times (Figure 6). The results of this experiment show that there is little correlation between the age of a peroxisome and its redox status (Figure 6; compare the 400/480 excitation ratios of roGFP2-PTS1 observed for the TMR-labeled organelles—which are at least 2 [Figure 6A], 5 [Figure 6B], or 6 d old [Figure 6C]—with those values obtained for the newly formed nonlabeled organelles). Figure 6E shows a fluorescence micrograph of a cell 5 d after pulse labeling with the HaloTag TMR ligand. Note that the 400/480 excitation ratio of roGFP2-PTS1 is significantly higher in COS-7/H-cat cells (0.258 ± 0.041) than in COS-7 cells (0.217 ± 0.030) or immortalized wild-type MEFs (0.218 ± 0.024) ($p < 0.0001$). The underlying mechanism for this phenomenon is not clear.

Because our data do not exclude the possibility that peroxisomes with a disturbed redox balance are quickly removed by autophagy, we also cultivated MEFs in the presence of 3-methyladenine, a compound that, among other antiproteolytic properties, blocks the autophagic degradation of peroxisomes in cultured mammalian cells (Huybrechts *et al.*, 2009). Under those conditions, the percentage of peroxisomes displaying a 400/480 excitation ratio larger than the mean plus the SD of the control condition dramatically increased over time (control, ±13%; 1 d, ±19%; 2 d, ±30%; 3 d, ±48%). The results obtained for cells grown in the presence of 3-methyladenine for 3 d are shown in detail in Figure 7. These data suggest that a disturbance in peroxisomal redox balance may function as a trigger for organelle degradation.

phenomenon (Supplemental Figure S2; for more details, see *Discussion*). These results further highlight the suitability of roGFP2-PTS1 as a peroxisomal redox indicator. In addition, they confirm that the intraperoxisomal redox status is strongly influenced by environmental growth conditions. Indeed it was recently shown that in the yeast *Pichia pastoris* the intraperoxisomal redox environment is more reductive in oleate-grown cells than in methanol-grown cells (Yano *et al.*, 2010).

Intraperoxisomal redox balance and cellular aging

Because it is well accepted that aging is associated with a general increase in oxidative stress (Muller, 2009), we investigated the influence of cell passage number on the redox balance of peroxisomes, mitochondria, and the cytosol in primary HuFs. Our results show that the redox state of peroxisomal and mitochondrial roGFP2 in late-passage cells was slightly, but significantly, higher ($p < 0.0001$)

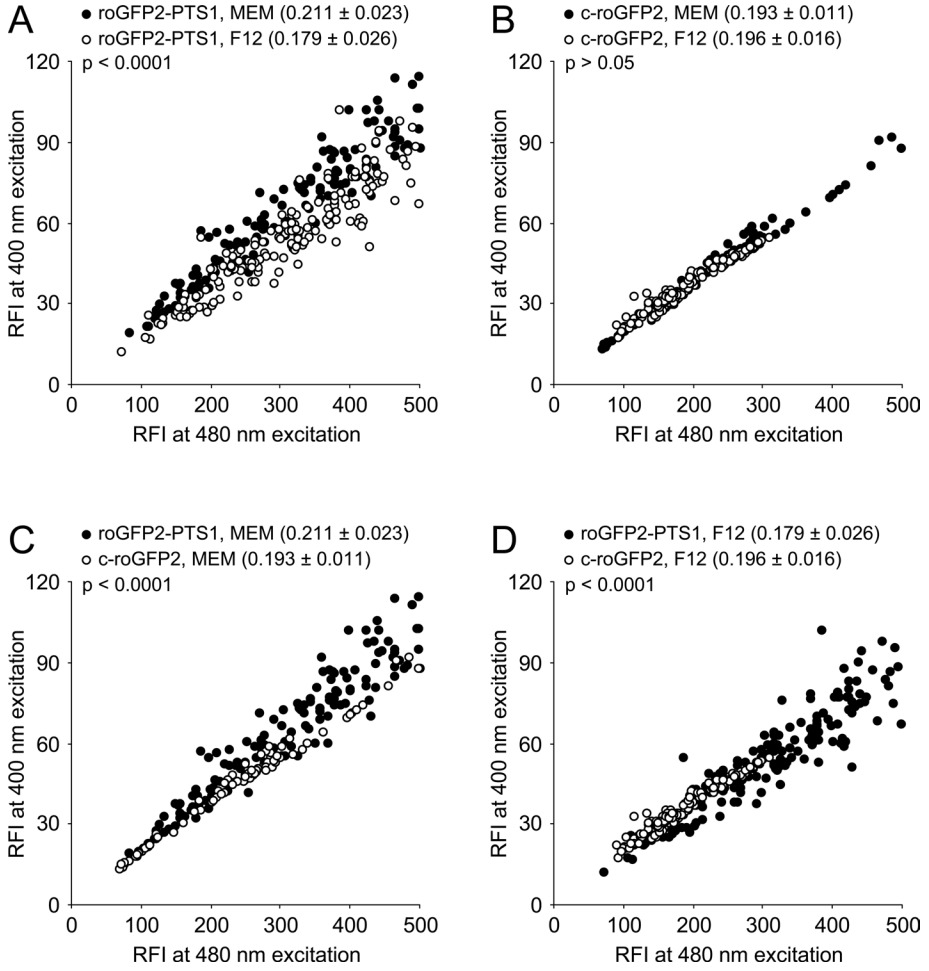

FIGURE 5: The intraperoxisomal redox environment is strongly influenced by the culture medium. Immortalized wild-type MEFs were transiently transfected with a plasmid encoding cytosolic (c-roGFP2) or peroxisomal (roGFP2-PTS1) roGFP2 and grown in standard growth medium (MEM) or Ham's F-12 nutrient medium. After 3 d, fluorescence micrographs of live cells were obtained and analyzed as described in *Materials and Methods*. The RFIs emitted from 400- and 480-nm excitation are plotted against each other. The numbers between brackets represent the average 400/480-nm excitation ratios (± SD). Each set of data was statistically compared.

than in early passage cells (Figure 8, A and C). The redox state of cytosolic roGFP2 was strongly increased in late-passage cells (Figure 8B). Note that roGFP2 in late-passage cells was even more oxidized in the cytosol (400/480-nm excitation ratio, 0.282 ± 0.055) than in the peroxisomal (400/480-nm excitation ratio, 0.246 ± 0.024) or mitochondrial (0.293 ± 0.059) matrices ($p < 0.005$). In line with previously published observations (Legakis *et al.*, 2002), we also observed that the number of peroxisomes per cell was sharply increased in late-passage cells (Supplemental Figure S3; compare upper and lower panels), and the majority of late-passage cells displayed a reduced capacity to import the roGFP2-PTS1 reporter protein (Supplemental Figure S3, middle panel).

Redox balance in the mitochondrial matrix is disturbed in catalase-deficient cells

Because there is evidence that catalase, a major peroxisomal enzyme responsible for the metabolism of H_2O_2, consumes H_2O_2 both produced in peroxisomes and created elsewhere in the cell (Koepke *et al.*, 2007, 2008), we investigated the oxidation state of roGFP2-PTS1, c-roGFP2, and mt-roGFP2 in immortalized wild-type and catalase-deficient MEFs (Ho *et al.*, 2004). We first confirmed the identity of these cell lines by immunofluorescence microscopy with anticatalase antibodies (Supplemental Figure S4A) and catalase activity measurements (Supplemental Figure S4B). Our roGFP2 measurements surprisingly revealed that the redox environment of the peroxisomal matrix was not increased in catalase-deficient cells (Figure 9A). This finding indicates that, under basal growth conditions, the amount of H_2O_2 generated at the level of peroxisomes can be detoxified by enzymes other than catalase (perhaps including glutathione peroxidase and PRDX5). Interestingly, the absence of catalase significantly increased the redox state of mitochondrial roGFP2 (Figure 9C). This effect was counteracted by forced reexpression of catalase (Figure 9D). The redox state of cytosolic roGFP2 was not notably different in wild-type as compared with catalase-deficient cells (Figure 9B). In summary, these observations support the idea that catalase plays an important role in the maintenance of mitochondrial redox balance, a notion already put forth (Koepke *et al.*, 2008).

To investigate whether or not the lack of changes in peroxisomal redox status in catalase knockout cells could be due to a compensatory activation of antioxidant mechanisms, we exposed wild-type MEFs to 3-amino-1,2,4-triazole (3-AT), a catalase inhibitor, and assayed the oxidation states of roGFP2-PTS1, mt-roGFP2, and c-roGFP2 as a function of time. Supplemental Figure S5 shows that acute catalase inhibition by 3-AT resulted in a small but significant ($p < 0.0001$) increase in the redox status of mt-roGFP2 but not roGFP2-PTS1. In addition, these experiments revealed a robust but transient burst of ROS in the cytosol, the significance of which is unclear. These findings are largely in line with the results obtained with catalase-deficient cells and suggest that the lack of an altered intraperoxisomal redox status in catalase-deficient cells is not due to an adaptive response.

RoGFP2-PTS1 can be used as a biosensor to detect KillerRed-PTS1–induced oxidative bursts

To induce oxidative stress in the peroxisomal matrix in a controlled spatiotemporal manner, we constructed a mammalian expression vector designed to append KSKL to KillerRed (KR-PTS1), a genetically encoded photosensitizer which produces singlet oxygen and superoxide radicals upon green light illumination (Bulina *et al.*, 2006; Carpentier *et al.*, 2009). The proper localization of KillerRed-PTS1 was confirmed by expressing the protein in control (WT) and Pex5p-deficient ($5^{-/-}$) mouse fibroblasts (Figure 1, A and B). Note that although KR-PTS1 and roGFP2-PTS1 share the same PTS1 sequence (in this case, KSKL), the proteins exhibited different import kinetics (Figure 1C). The mechanism underlying this effect remains to be investigated. To determine whether KR-PTS1–induced oxidative bursts can be monitored by roGFP2-PTS1, we coexpressed both

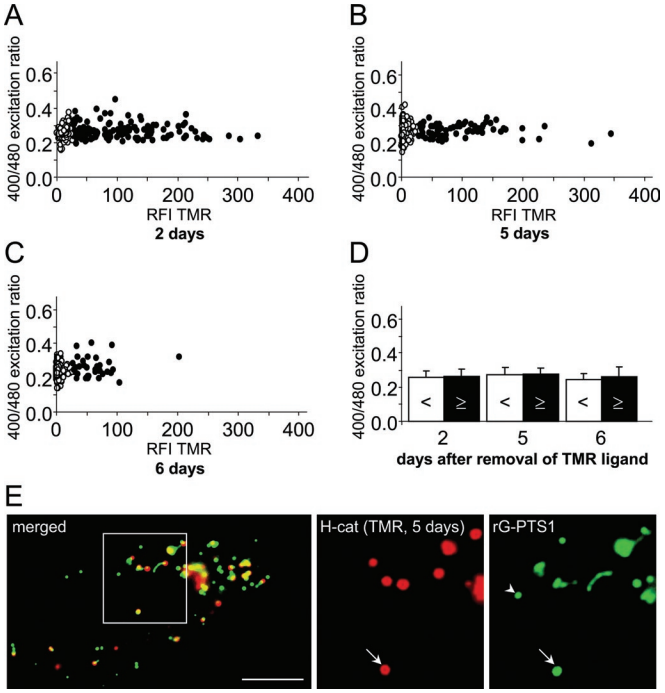

FIGURE 6: The redox state of roGFP2-PTS1 is not correlated with peroxisome age. COS-7 cells stably expressing HaloTag-catalase (H-cat) were pulse labeled with the red-colored HaloTag TMR (TMR) ligand. After removal of the ligand, the cells were transiently transfected with a plasmid coding for roGFP2-PTS1 (rG-PTS1) and cultivated in standard growth medium. Fluorescence micrographs were taken after 2, 5, and 6 d, and the images were analyzed as described in *Materials and Methods*. (A–C) The 400/480-nm excitation ratios of individual peroxisomes are plotted against the RFIs of the corresponding TMR signals. TMR-negative and TMR-positive organelles are indicated by black open and solid circles, respectively (arbitrary cutoff value, RFI = 25). (D) The ratio values represent the mean ± SD. <, peroxisomes younger than the day indicated; ≥, peroxisomes formed before or on the day indicated. (E) Representative fluorescence micrograph of a cell 5 d after pulse labeling with the HaloTag TMR ligand. The arrow and arrowhead indicate an "old" and a "young" peroxisome, respectively.

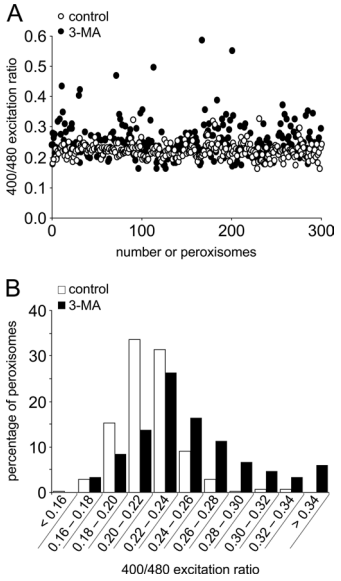

FIGURE 7: Effect of 3-methyladenine on the redox state of roGFP2-PTS1 in individual peroxisomes. Immortalized wild-type MEFs were transiently transfected with a plasmid encoding roGFP2-PTS1 and grown in standard growth medium (MEM). The next day, the cells were cultivated in MEM supplemented (3-MA) or not (control) with 10 mM 3-methyladenine. Three days later, fluorescence micrographs were taken and 300 randomly chosen peroxisomes (from at least 10 different cells) were analyzed as described in *Materials and Methods*. The 400/480-nm excitation ratios are (A) plotted and (B) presented in a relative-frequency histogram.

proteins in wild-type MEFs and artificially induced oxidative stress in the peroxisomal matrix through green light irradiation. These experiments showed that 1) roGFP2-PTS1 rapidly responds to KR-PTS1–mediated ROS production, 2) the oxidation of roGFP2-PTS1 is KR-PTS1 and light dose dependent, and 3) peroxisomal roGFP2 does not recover from the oxidative insult within the time frame examined (Figure 10).

Peroxisome-derived oxidative stress disturbs mitochondrial redox balance

To gain additional insight into interorganellar cross-talk and oxidative stress, we investigated whether the subcellular location of KillerRed-mediated ROS production has any effect on the intraperoxisomal redox state. Our results demonstrate that, within limits, peroxisomes resist oxidative stress generated in the cytosol or mitochondria, but they are affected when the stress originates within the organelle (Figure 11A). We also assayed the response of cytosolic roGFP2 to peroxisome-, mitochondria-, and cytosol-derived oxidative stress. These experiments revealed that the oxidative state of c-roGFP2 was hardly affected under the conditions used, even when cytosolic KillerRed (c-KR) was expressed (Figure 11B). However, it should be noted that the KillerRed concentrations (expressed as the relative fluorescence intensities of the photosensitizer per unit area [μm^2]; n = 50) in the cytosolic compartment (4953 ± 2103) were considerably lower than the concentrations found in the peroxisomal (21,921 ± 9750) and mitochondrial (31,375 ± 4633) compartments. Finally, we examined the effect of peroxisome-, cytosol-, and mitochondria-derived oxidative stress on the redox state of the mitochondrial matrix. Here it was clear that generating excess ROS inside each compartment quickly disturbed the mitochondrial redox balance, albeit to different extents (Figure 11C). Importantly, these conditions resulted in excessive mitochondrial fragmentation (Supplemental Figure S6, A–C). Note that 1) these fragmentation events were KillerRed dependent (Supplemental Figure S6A, compare left top and bottom cell), 2) none of the conditions affected peroxisome morphology (Bulina *et al.*, 2006), and 3) KillerRed fluorescence was quickly quenched upon green light illumination (Figure 11D; Supplemental Figure S6, A–C: compare the images taken at time 0 and after 4 min).

DISCUSSION

In this study, we investigated the usefulness of roGFP2-PTS1, a peroxisomal variant of the redox-sensitive EGFP derivative, to monitor the intraperoxisomal dithiol–disulfide equilibrium in the context of living mammalian cells. Our results show that roGFP2-PTS1 is sufficiently sensitive to detect changes in the peroxisomal redox environment in response to altered growth conditions or upon challenge with cell-permeant oxidants and reductants, toxicologically relevant metal ions, or green light illumination after KillerRed-PTS1 expression. Collectively, these observations demonstrate the suitability of roGFP2-PTS1 as an intraperoxisomal redox indicator in mammalian cells.

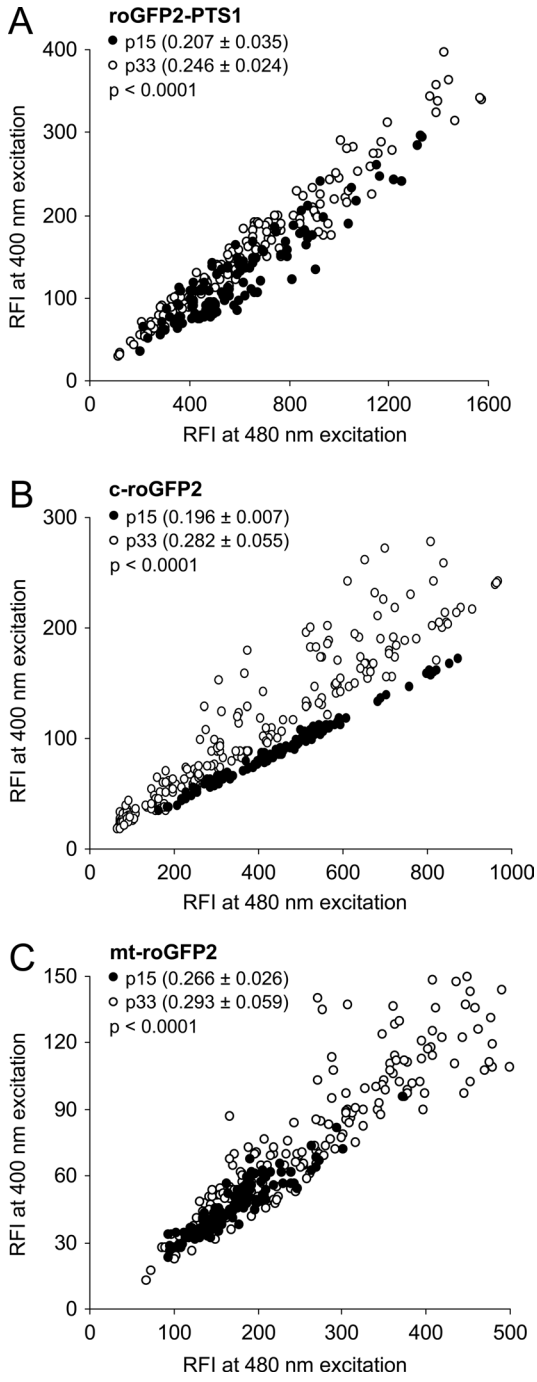

FIGURE 8: The oxidation states of roGFP2-PTS1, c-roGFP2, and mt-roGFP2 increase during cellular aging. Primary human fibroblasts (passage 15 or 31) were transiently transfected with a plasmid encoding (A) peroxisomal (roGFP2-PTS1), (B) cytosolic (c-roGFP2), or (C) mitochondrial (mt-roGFP2) roGFP2 and grown in standard growth medium (MEM). After 2 d, fluorescence micrographs of live cells were obtained and analyzed as described in *Materials and Methods*. The RFIs emitted from 400- and 480-nm excitation are plotted against each other. The numbers between brackets represent the average 400/480-nm excitation ratios (± SD). Each set of data was statistically compared and differences exist at $p < 0.0001$.

Our efforts resulted in the somewhat surprising finding that cultivating cells in the presence of ascorbic acid, a common culture medium and dietary supplement known for its antioxidant properties (Osiecki *et al.*, 2010), actually increased the oxidation of peroxisomal roGFP2. However, it should be noted that under select conditions ascorbic acid is known to also function as a prooxidant (Osiecki *et al.*, 2010). For example, it was reported that pharmacological doses of ascorbic acid increase lipid peroxide content in rat pheochromocytoma cells (Song *et al.*, 2001) and generate H_2O_2-dependent cytotoxicity in a variety of cancer cells (Chen *et al.*, 2008; Cheung *et al.*, 2010).

Currently there is considerable interest in how peroxisomes contribute to cellular ROS levels, redox signaling, and oxidative balance or damage in human metabolism (Titorenko and Terlecky, 2011). The combined use of targeted KillerRed and roGFP2 proteins allowed us to locally increase and measure ROS levels in different subcellular compartments. Our data are in line with previous observations that the ROS-induced phototoxicity of KillerRed is location dependent (Bulina *et al.*, 2006).

Using these powerful tools, we were able to confirm and extend previous observations concerning the redox-sensitive relationship between peroxisomes and mitochondria. For example, we found that generating ROS inside peroxisomes disturbs the mitochondrial redox balance, which may lead to excessive mitochondrial fragmentation. These findings suggest that peroxisomes may act as an upstream initiator of mitochondrial ROS signaling pathways. This finding strengthens the view that the peroxisome is not solely a metabolic organelle but also an intracellular signaling compartment that promotes developmental decisions (Titorenko and Rachubinski, 2004; Dixit *et al.*, 2010). In this context, we also note that loss of peroxisome function triggers necrosis in *Saccharomyces cerevisiae* (Jungwirth *et al.*, 2008), and the absence of the peroxisomal peroxiredoxin PRDX5 leads to necrotic cell death in *Hansenula polymorpha* (Aksam *et al.*, 2008). We also found that mitochondria of catalase-deficient cells experienced a significant loss of redox balance. Curiously, peroxisomes themselves in these cells maintained oxidative equilibrium. Therefore, peroxisomes of catalase-deficient cells have a mechanism of either efficiently metabolizing intraorganellar ROS or thwarting their production—possibilities considered further in this paper.

Catalase's precise role in cellular redox balance remains a topic of great interest and debate. Inactivation of peroxisomal catalase has been linked to a shorter life span in *Caenorhabditis elegans* and *S. cerevisiae* (Petriv and Rachubinski, 2004), yet mice completely deficient in the enzyme develop normally and are apparently healthy (Ho *et al.*, 2004). Catalase inactivation with 3-AT is progeric in human cells (Wood *et al.*, 2006) yet it elicits a hormetic, life span–extending phenotype in *S. cerevisiae* (Mesquita *et al.*, 2010). Furthermore, in human populations, the absence of peroxisomal catalase causes effects that vary from the relatively benign to disabling and life threatening. From a mechanistic standpoint, it is not clear how this antioxidant enzyme, which is predominantly localized in peroxisomes of mammalian cells, can reduce the harmful effects of H_2O_2 generated in mitochondria. Several explanations may be put forth.

One is that mitochondria in wild-type cells have low levels of this enzyme (Radi *et al.*, 1991). However, because mammalian catalases lack any recognizable mitochondrial targeting sequences and we never observed endogenous or heterologously expressed catalase in mitochondria of mammalian cells (unpublished data), this is unlikely. Alternatively, because H_2O_2 is freely diffusible through mammalian cell membranes (Koopman *et al.*, 2010), it is tempting to speculate that peroxisomal catalase directly contributes to the degradation of H_2O_2 released by mitochondria. However, because 1) intramitochondrial H_2O_2 production is virtually completely counteracted by mitochondrial peroxiredoxins and glutathione peroxidases (Cox *et al.*, 2010), 2) the range of action of each ROS is

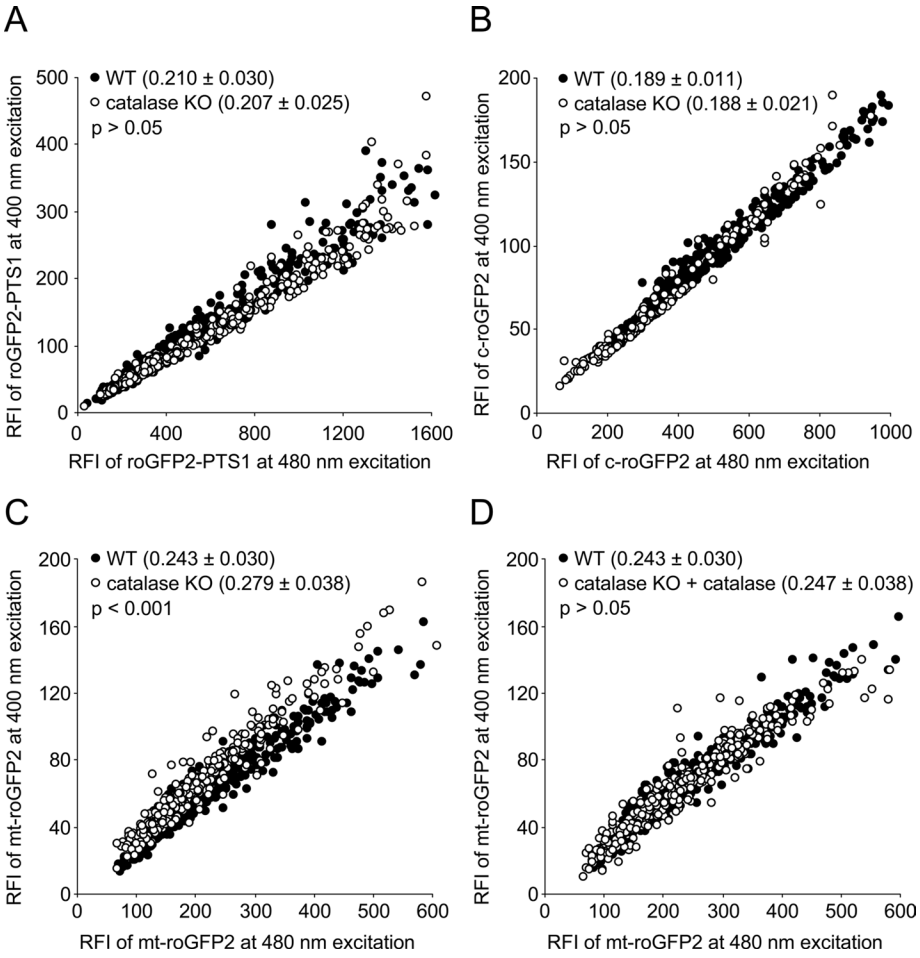

FIGURE 9: Knocking out catalase activity disturbs the intracellular redox balance. Immortalized wild-type (WT) and catalase-deficient (catalase KO) MEFs were transiently transfected with a plasmid encoding (A) peroxisomal roGFP2 (roGFP2-PTS1), (B) cytosolic roGFP2 (c-roGFP2), (C) mitochondrial roGFP2 (mt-roGFP2), or (D) mt-roGFP2 and catalase, and cultivated in standard growth medium. After 2 d, fluorescence micrographs of live cells were obtained and analyzed as described in *Materials and Methods*. The RFIs emitted from 400- and 480-nm excitation are plotted against each other. Each set of data was statistically compared ($p > 0.05$ was not considered a significant difference; $p < 0.001$ was considered a significant difference).

codetermined by its free aqueous diffusion distance, which appears to have an upper limit of 0.23–0.46 μm for H_2O_2 (Forkink *et al.*, 2010; Koopman *et al.*, 2010), and 3) the redox state of cytosolic roGFP2 was not notably different in wild-type as compared with catalase-deficient cells, this possibility has limitations. A third explanation is that the inactivation of catalase affects peroxisomal metabolism (Hashimoto and Hayashi, 1987; Sheikh *et al.*, 1998; Titorenko and Terlecky, 2011). This may trigger signaling and communication events that ultimately result in increased mitochondrial stress. This could be ROS mediated or, perhaps, metabolite mediated.

Peroxisomes and mitochondria exhibit a functional interplay that continues to emerge. Linking the organelles is oxidative metabolism of specific fatty acids, which are initially processed in peroxisomes and then trafficked to mitochondria where reactions are completed (Van Veldhoven, 2010). The organelles also communicate via anaplerotic metabolism—metabolites formed in the peroxisome replenish needed biochemical substrates (e.g., tricarboxylic acid intermediates) in the mitochondria (reviewed by Titorenko and Terlecky, 2011). It could be envisioned that as peroxisomal metabolism is slowed in specific pathological circumstances, critical metabolic intermediates (e.g., acetyl-CoA) are not properly (produced and) trafficked to mitochondria. If mitochondrial metabolism is similarly disrupted, an increase in uncoupled reactions and ROS production could certainly be anticipated. Note that loss of catalase activity or KillerRed-mediated ROS production inside peroxisomes may initiate lipid peroxidation of the organelle membrane, thereby altering its physical properties and affecting (peroxisome) biogenesis and metabolism.

Peroxisomal dysfunction has been shown to be linked to cellular aging (Terlecky *et al.*, 2006; Koepke *et al.*, 2007). Here we showed that aging primary human skin fibroblasts in cellulo shifts the peroxisomal, mitochondrial, and cytosolic redox balance to a more oxidized state. This finding is in line with the general idea that aged cells display an elevated prooxidant state due to increased oxidant production and a decline in antioxidant defenses (Hagen, 2003). For example, it was shown that γ-glutamylcysteine synthetase, the rate-limiting enzyme in the synthesis of glutathione (GSH), displays a marked age-related decrease in enzyme activity (Hagen, 2003). Previous work has indicated that roGFP2 preferentially acts as a sensor for the glutathione redox potential (Schwarzländer *et al.*, 2008), so it is interesting to note that 1) the strongest increase in redox stress was observed in the cytosol, the subcellular location where GSH synthesis occurs, and 2) incubating MEFs for 22 h in medium containing 100 μM L-buthionine-(S,R)-sulfoximine (Griffith and Meister, 1979), a potent inhibitor of γ-glutamylcysteine synthetase, significantly increased the redox state of mitochondrial and cytosolic roGFP2 ($p < 0.0001$) but not peroxisomal roGFP2 ($p = 0.453$). These findings suggest that peroxisomes may possess their own GSH pool. This idea is further corroborated by our observation that the dithiol–disulfide equilibrium in individual peroxisomes is nonuniform, even within a single cell. This observation is in line with the previous finding that the peroxisomal membrane forms a permeability barrier in vivo (Visser *et al.*, 2007).

The aim of this study was to gain a better insight into how peroxisomes contribute to the maintenance of extraperoxisomal ROS levels within mammalian cells and how these cells cope with peroxisome-derived ROS. It is clear from this work that peroxisomes and mitochondria functionally interact—presumably via ROS, metabolites, substrates, or perhaps through other yet-to-be-identified factors. Further characterization of these interactions and their mediators is crucial for understanding the physiological relevance of these organelles in cellular aging and the initiation and progression of age-related diseases.

MATERIALS AND METHODS

DNA manipulations and plasmids

The mammalian expression vectors pEGFP-N1 (Clontech, Mountain View, CA) and pKillerRed-dmito (Bio-Connect, Huissen, The Netherlands) were commercially obtained. The yeast expression

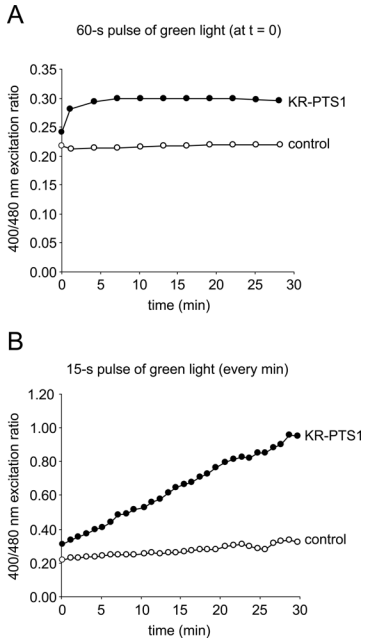

FIGURE 10: RoGFP2-PTS1 can be used to detect KillerRed-PTS1–induced oxidative bursts. Immortalized wild-type MEFs were transiently transfected with plasmids encoding roGFP2-PTS1 alone (control) or together with KillerRed-PTS1 (KR-PTS1) and cultivated in standard growth medium. After 3 d, the cells were exposed to (A) one 60-s pulse or (B) 30 sequential 15-s pulses of green light. Fluorescence micrographs were taken at the indicated time points and analyzed as described in *Materials and Methods*. The relative fluorescence intensities emitted from 400- and 480-nm excitation were used to calculate the 400/480-nm excitation ratios. Representative results from one of three experiments are shown.

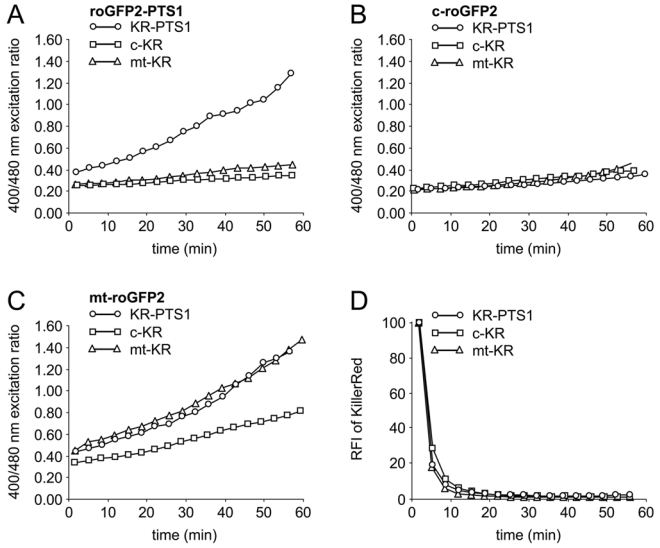

FIGURE 11: KillerRed-mediated redox signaling from and to peroxisomes. Immortalized wild-type MEFs were transiently cotransfected with plasmids encoding peroxisomal (roGFP2-PTS1), cytosolic (c-roGFP2), or mitochondrial (mt-roGFP2) roGFP2, and peroxisomal (KR-PTS1), cytosolic (c-KR), or mitochondrial (mt-KR) KillerRed. After 3 d, the cells were exposed every 200 s to a 15-s pulse of green light. Fluorescence micrographs were taken at the indicated time points and analyzed as described in *Materials and Methods*. (A–C) The relative fluorescence intensities emitted from 400- and 480-nm excitation were used to calculate the 400/480-nm excitation ratios (representative results from one of three experiments are shown). (D) Representative photobleaching curves for the KillerRed proteins. RFI, relative fluorescence intensity. The typical fluorescence pattern of each reporter protein is shown in Supplemental Figure S1.

vector encoding eroGFP (ER-targeted redox-sensitive GFP) (Merksamer *et al.*, 2008) was obtained from P. Agostinis (K.U. Leuven, Leuven, Belgium). Oligonucleotides (Supplementary Table 1) were synthesized by Integrated DNA Technologies (Leuven, Belgium). PCR applications were performed routinely using *Pfx* DNA polymerase (Invitrogen). Restriction enzymes were purchased from TaKaRa (Lonza, Verviers, Belgium). The *Escherichia coli* strain *Top10F'* (Invitrogen, Merelbeke, Belgium) was used for all DNA manipulations. The plasmid encoding roGFP2-PTS1 (pMF1706) was constructed by amplifying the roGFP2 cDNA fragment by PCR (template, eroGFP; primers, pEGFPfwHindIII and pIRES_GFPSKLRvNotI) and cloning the *Hind*III/*Not*I–digested PCR product into the backbone fragment of *Hind*III/*Not*I–restricted pEGFP-N1. The construct encoding cytosolic roGFP2 (pMF1707) was generated in an identical manner by employing the primers pEGFPfwHindIII and EGFP-NotIrv. The construct coding for mitochondrial roGFP2 (pMF1762) was generated by ligating the *Bgl*II/*Not*I roGFP-encoding fragment of pMF1707 to the *Bam*HI/*Not*I–digested backbone fragment of pKillerRed-dmito. The plasmid encoding KillerRed-PTS1 (pMF1754) was generated by amplifying the KillerRed cDNA fragment by PCR (template, pKillerRed-dmito; primers, KillerRedfwBglII and KillerRedKSKLrvNotI) and cloning the *Bgl*II/*Not*I–digested PCR product into the backbone fragment of *Bgl*II/*Not*I–restricted pEGFP-N1. The construct encoding cytosolic KillerRed (pMF1755) was generated in an identical manner by employing the primers KillerRedfwBglII and KillerRedrvNotI. The mammalian expression plasmid encoding nontagged human catalase was generated by ligating the PCR-amplified catalase cDNA fragment (template pJK19 [Legakis *et al.*, 2002]; primers, HsCatalase.1fwBglII and pBADHisrvNotIPstI; digested with *Bgl*II/*Pst*I) into the *Bgl*II/*Pst*I–restricted pEGFP-N1 vector. All plasmids were verified by DNA sequencing (Agowa, Berlin, Germany).

Statistical analysis

Statistics were performed by using VassarStats, a website for statistical computation (http://faculty.vassar.edu/lowry//VassarStats.html). One-way analysis of variance was used to determine the differences among independent groups of numerical values, and individual differences were further explored with a Student's *t* test. The significance level was chosen to be 0.05.

Cell culture, transfections, and (immuno)fluorescence microscopy

The Pex16p-deficient human fibroblasts were obtained from Coriell Cell Repositories (Camden, NJ). Control human fibroblasts were kindly provided by D. Cassiman (K.U. Leuven, Leuven, Belgium). Control MEFs (C57BL/6) were generated by P. Van Veldhoven. The Pex5$^{-/-}$ MEFs, the catalase$^{-/-}$ MEFs (C57BL/6), and the COS-7 cells expressing HaloTag catalase are described elsewhere (Baes *et al.*, 1997; Ho *et al.*, 2004; Delille *et al.*, 2010). All MEFs were immortalized by introduction of the SV40 large T-antigen. Unless specified otherwise, all cells were cultured at 37°C in a humidified 5% CO_2 incubator in MEM Eagle alpha (BioWhittaker; catalogue no. 12-169; Lonza, Verviers, Belgium) supplemented with 10% (vol/vol) heat-inactivated South American

fetal calf serum (Invitrogen), 2 mM Glutamax (Invitrogen), antibiotic-antimycotic mixture (Invitrogen) (100 μg/ml penicillin G, 100 μg/ml streptomycin sulfate, 0.25 μg/ml amphotericin B), and 5 μg/ml plasmocin (Amaxa; Lonza, Verviers, Belgium). The F-12 nutrient mixture containing L-glutamine was from Invitrogen (catalogue no. 11765-054). Cells were transfected by employing the Neon Transfection System (Invitrogen; MEFs: 1350 V, 30-ms pulse width, 1 pulse; COS-7 cells: 1050 V, 30-ms pulse width, 2 pulses; HuFs: 1300 V, 30-ms pulse width, 1 pulse). In vivo pulse labeling of COS-7 cells stably expressing HaloTag catalase with the cell-permeable HaloTag TMR ligand (final concentration 250 nM; Promega, Leiden, The Netherlands) was performed as described (Delille *et al.*, 2010). Samples for immunofluorescence microscopy were fixed and processed as described (Huybrechts *et al.*, 2009). Cells for live-cell imaging were seeded and imaged in FD-35 Fluorodish cell culture dishes (World Precision Instruments, Hertfordshire, England). Fluorescence was evaluated on a motorized inverted IX-81 microscope, controlled by Cell-M software and equipped with 1) a temperature, humidity, and CO_2-controlled incubation chamber; 2) a 100× Super Apochromat oil immersion objective; 3) BP360–370, BP470–495, BP545–580, and D405/20x excitation filters; 4) BA420–460, BA510–550, and BA610IF emission filters; and 5) a CCD-FV2T digital black and white camera (Olympus, Aartselaar, Belgium). The camera exposure time was set to 500 and 100 ms to acquire roGFP2 images at 400- and 480-nm excitation wavelengths, respectively. To generate KillerRed-mediated ROS, the cells were irradiated with green light (100× oil objective, 545–580 nm, 1300 μW/cm^2) for the indicated time frames. The Olympus image analysis and particle detection software were used for quantitative image analysis. To quantify the relative fluorescence intensities (RFIs) of individual peroxisomes or mitochondria, the organelles were selected by employing the circle region-of-interest tool (surface area, 0.3–0.5 μm^2). H_2O_2 concentrations in cell culture supernatants were determined by using titanyl sulfate, modified from Baudhuin *et al.* (1964).

ACKNOWLEDGMENTS

We thank M. Baes (Katholieke Universiteit Leuven, Leuven, Belgium) for the Pex5p-deficient mouse embryonic fibroblasts, P. Agostinis (Katholieke Universiteit Leuven, Leuven, Belgium) for the roGFP2 DNA template, S. Subramani (University of California, San Diego, San Diego, CA) for the plasmid encoding the SV40 large T-antigen, and W. Deckers (Olympus Belgium) for measuring the green light intensity emitted by the light source of our live-cell imaging station. This work is supported by grants from the "Fonds voor Wetenschappelijk Onderzoek-Vlaanderen (Onderzoeksproject G.0754.09)" and the "Bijzonder Onderzoeksfonds van de K.U.Leuven (OT/09/045)."

REFERENCES

Aksam BE, Jungwirth H, Kohlwein SD, Ring J, Madeo F, Veenhuis M, Van Der Klei IJ (2008). Absence of the peroxiredoxin Pmp20 causes peroxisomal protein leakage and necrotic cell death. Free Radic Biol Med 45, 1115–1124.

Antonenkov VD, Grunau S, Ohlmeier S, Hiltunen JK (2010). Peroxisomes are oxidative organelles. Antioxid Redox Signal 13, 525–537.

Baes M *et al.* (1997). A mouse model for Zellweger syndrome. Nat Genet 17, 49–57.

Baudhuin P, Beaufay H, Rahman-Li Y, Sellinger OZ, Wattiaux R, Jacques P, de Duve C (1964). Tissue fractionation studies. 17. Intracellular distribution of monoamine oxidase, aspartate aminotransferase, alanine aminotransferase, D-amino acid oxidase and catalase in rat-liver tissue. Biochem J 92, 179–184.

Bonekamp NA, Völkl A, Fahimi HD, Schrader M (2009). Reactive oxygen species and peroxisomes: struggling for balance. Biofactors 35, 346–355.

Bulina ME, Chudakov DM, Britanova OV, Yanushevich YG, Staroverov DB, Chepurnykh TV, Merzlyak EM, Shkrob MA, Lukyanov S, Lukyanov KA (2006). A genetically encoded photosensitizer. Nat Biotechnol 24, 95–99.

Carpentier P, Violot S, Blanchoin L, Bourgeois D (2009). Structural basis for the phototoxicity of the fluorescent protein KillerRed. FEBS Lett 583, 2839–2842.

Casey JR, Grinstein S, Orlowski J (2010). Sensors and regulators of intracellular pH. Nat Rev Mol Cell Biol 11, 50–61.

Chen Q, Espey MG, Sun AY, Pooput C, Kirk KL, Krishna MC, Khosh DB, Drisko J, Levine M (2008). Pharmacologic doses of ascorbate act as a prooxidant and decrease growth of aggressive tumor xenografts in mice. Proc Natl Acad Sci USA 105, 11105–11109.

Cheung FW, Che CT, Sakagami H, Kochi M, Liu WK (2010). Sodium 5,6-benzylidene-L-ascorbate induces oxidative stress, autophagy, and growth arrest in human colon cancer HT-29 cells. J Cell Biochem 111, 412–424.

Circu ML, Aw TY (2010). Reactive oxygen species, cellular redox systems, and apoptosis. Free Radic Biol Med 48, 749–762.

Cox AG, Winterbourn CC, Hampton MB (2010). Mitochondrial peroxiredoxin involvement in antioxidant defence and redox signalling. Biochem J 425, 313–325.

de Duve C, Baudhuin P (1966). Peroxisomes (microbodies and related particles). Physiol Rev 46, 323–357.

Delille HK, Agricola B, Guimaraes SC, Borta H, Lüers GH, Fransen M, Schrader M (2010). Pex11pβ-mediated growth and division of mammalian peroxisomes follows a maturation pathway. J Cell Sci 123, 2750–2762.

Dixit E *et al.* (2010). Peroxisomes are signaling platforms for antiviral innate immunity. Cell 141, 668–681.

Dooley CT, Dore TM, Hanson GT, Jackson WC, Remington SJ, Tsien RY (2004). Imaging dynamic redox changes in mammalian cells with green fluorescent protein indicators. J Biol Chem 279, 22284–22293.

Dowling DK, Simmons LW (2009). Reactive oxygen species as universal constraints in life-history evolution. Proc Biol Sci 276, 1737–1745.

Fialkow L, Wang Y, Downey GP (2007). Reactive oxygen and nitrogen species as signaling molecules regulating neutrophil function. Free Radic Biol Med 42, 153–164.

Forkink M, Smeitink JA, Brock R, Willems PH, Koopman WJ (2010). Detection and manipulation of mitochondrial reactive oxygen species in mammalian cells. Biochim Biophys Acta 1797, 1034–1044.

Góth L, Eaton JW (2000). Hereditary catalase deficiencies and increased risk of diabetes. Lancet 356, 1820–1821.

Griffith O, Meister A (1979). Potent and specific inhibition of glutathione synthesis by buthionine sulfoximine (S-n-butyl homocysteine sulfoximine). J Biol Chem 254, 7558–7560.

Hagen TM (2003). Oxidative stress, redox imbalance, and the aging process. Antioxid Redox Signaling 5, 503–506.

Hanson GT, Aggeler R, Oglesbee D, Cannon M, Capaldi RA, Tsien RY, Remington SJ (2004). Investigating mitochondrial redox potential with redox-sensitive green fluorescent protein indicators. J Biol Chem 279, 13044–13053.

Hanson GT, McAnaney TB, Park ES, Rendell ME, Yarbrough DK, Chu S, Xi L, Boxer SG, Montrose MH, Remington SJ (2002). Green fluorescent protein variants as ratiometric dual emission pH sensors. 1. Structural characterization and preliminary application. Biochemistry 41, 15477–15488.

Hashimoto F, Hayashi H (1987). Significance of catalase in peroxisomal fatty acyl-CoA beta-oxidation. Biochim Biophys Acta 921, 142–150.

Henkler F, Brinkmann J, Luch A (2010). The role of oxidative stress in carcinogenesis induced by metals and xenobiotics. Cancers 2, 376–396.

Ho YS, Xiong Y, Ma W, Spector A, Ho DS (2004). Mice lacking catalase develop normally but show differential sensitivity to oxidant tissue injury. J Biol Chem 279, 32804–32812.

Honsho M, Tamura S, Shimozawa N, Suzuki Y, Kondo N, Fujiki Y (1998). Mutation in *PEX16* is causal in the peroxisome-deficient Zellweger syndrome of complementation group D. Am J Hum Genet 63, 1622–1630.

Huybrechts SJ, Van Veldhoven PP, Brees C, Mannaerts GP, Los GV, Fransen M (2009). Peroxisome dynamics in cultured mammalian cells. Traffic 10, 1722–1733.

Jungwirth H, Ring J, Mayer T, Schauer A, Büttner S, Eisenberg T, Carmona-Gutierrez D, Kuchler K, Madeo F (2008). Loss of peroxisome function triggers necrosis. FEBS Lett 582, 2882–2886.
Karlsson M, Kurz T, Brunk UT, Nilsson SE, Frennesson CI (2010). What does the commonly used DCF test for oxidative stress really show? Biochem J 428, 183–190.
Kasai H, Okada Y, Nishimura S, Rao MS, Reddy JK (1989). Formation of 8-hydroxydeoxyguanosine in liver DNA of rats following long-term exposure to a peroxisome proliferator. Cancer Res 49, 2603–2605.
Koepke JI, Nakrieko KA, Wood CS, Boucher KK, Terlecky LJ, Walton PA, Terlecky SR (2007). Restoration of peroxisomal catalase import in a model of human cellular aging. Traffic 8, 1590–1600.
Koepke JI, Wood CS, Terlecky LJ, Walton PA, Terlecky SR (2008). Progeric effects of catalase inactivation in human cells. Toxicol Appl Pharmacol 232, 99–108.
Koopman WJ, Nijtmans LG, Dieteren CE, Roestenberg P, Valsecchi F, Smeitink JA, Willems PH (2010). Mammalian mitochondrial complex I: biogenesis, regulation, and reactive oxygen species generation. Antioxid Redox Signaling 12, 1431–1470.
Lametschwandtner G, Brocard C, Fransen M, Van Veldhoven P, Berger J, Hartig A (1998). The difference in recognition of terminal tripeptides as peroxisomal targeting signal 1 between yeast and human is due to different affinities of their receptor Pex5p to the cognate signal and to residues adjacent to it. J Biol Chem 273, 33635–33643.
Legakis JE, Koepke JI, Jedeszko C, Barlaskar F, Terlecky LJ, Edwards HJ, Walton PA, Terlecky SR (2002). Peroxisome senescence in human fibroblasts. Mol Biol Cell 13, 4243–4255.
Mammucari C, Rizzuto R (2010). Signaling pathways in mitochondrial dysfunction and aging. Mech Ageing Dev 131, 536–543.
Merksamer PI, Trusina A, Papa FR (2008). Real-time redox measurements during endoplasmic reticulum stress reveal interlinked protein folding functions. Cell 135, 933–947.
Mesquita A, Weinberger M, Silva A, Sampaio-Marques B, Almeida B, Leão C, Costa V, Rodrigues F, Burhans WC, Ludovico P (2010). Caloric restriction or catalase inactivation extends yeast chronological lifespan by inducing H_2O_2 and superoxide dismutase activity. Proc Natl Acad Sci USA 107, 15123–15128.
Meyer AJ, Dick TP (2010). Fluorescent protein-based redox probes. Antioxid Redox Signaling 13, 621–650.
Morel F, Rauch C, Petit E, Piton A, Theret N, Coles B, Guillouzo A (2004). Gene and protein characterization of the human glutathione S-transferase kappa and evidence for a peroxisomal localization. J Biol Chem 279, 16246–16253.
Muller M (2009). Cellular senescence: molecular mechanisms, in vivo significance, and redox considerations. Antioxid Redox Signaling 11, 59–98.
Oakly AJ (2005). Glutathione transferases: new functions. Curr Opin Struct Biol 15, 716–723.
Osiecki M, Ghanavi P, Atkinson K, Nielsen LK, Doran MR (2010). The ascorbic acid paradox. Biochem Biophys Res Commun 400, 466–470.
Petriv OI, Rachubinski RA (2004). Lack of peroxisomal catalase causes a progeric phenotype in *Caenorhabditis elegans*. J Biol Chem 279, 19996–20001.
Radi R, Turrens JF, Chang LY, Bush KM, Crapo JD, Freeman BA (1991). Detection of catalase in rat heart mitochondria. J Biol Chem 266, 22028–22034.
Reddy JK, Lalwani ND, Reddy MK, Qureshi SA (1982). Excessive accumulation of autofluorescent lipofuscin in the liver during hepatocarcinogenesis by methyl clofenapate and other hypolipidemic peroxisome proliferators. Cancer Res 42, 259–266.
Roberts CK, Sindhu KK (2009). Oxidative stress and metabolic syndrome. Life Sci 84, 705–712.
Salmon AB, Richardson A, Pérez VI (2010). Update on the oxidative stress theory of aging: does oxidative stress play a role in aging or healthy aging? Free Radic Biol Med 48, 642–655.
Schrader M, Fahimi HD (2006). Peroxisomes and oxidative stress. Biochim Biophys Acta 1763, 1755–1766.
Schwarzländer M, Fricker MD, Müller C, Marty L, Brach T, Novak J, Sweetlove LJ, Hell R, Meyer AJ (2008). Confocal imaging of glutathione redox potential in living plant cells. J Microsc 231, 299–316.
Schwarzländer M, Fricker MD, Sweetlove LJ (2009). Monitoring the in vivo redox state of plant mitochondria: effect of respiratory inhibitors, abiotic stress and assessment of recovery from oxidative challenge. Biochim Biophys Acta 1787, 468–475.
Sheikh FG, Pahan K, Khan M, Barbosa E, Singh I (1998). Abnormality in catalase import into peroxisomes leads to severe neurological disorder. Proc Natl Acad Sci USA 95, 2961–2966.
Song JH, Shin SH, Wang W, Ross GM (2001). Involvement of oxidative stress in ascorbate-induced proapoptotic death of PC12 cells. Exp Neurol 169, 425–437.
Suga T (2004). Hepatocarcinogenesis by peroxisome proliferators. J Toxicol Sci 1, 1–12.
Takahara S (1952). Progressive oral gangrene probably due to lack of catalase in the blood (acatalasemia); report of nine cases. Lancet 2, 1101–1104.
Takahara S, Miyamoto H (1948). Three cases of progressive oral gangrene due to lack of catalase in the blood. Jpn J Otol 51, 163–168.
Terlecky SR, Koepke JI, Walton PA (2006). Peroxisomes and aging. Biochim Biophys Acta 1763, 1749–1754.
Titorenko VI, Rachubinski RA (2004). The peroxisome: orchestrating important developmental decisions from inside the cell. J Cell Biol 164, 641–645.
Titorenko VI, Terlecky SR (2011). Peroxisome metabolism and cellular aging. Traffic 12, 252–259.
Van Veldhoven PP (2010). Biochemistry and genetics of inherited disorders of peroxisomal fatty acid metabolism. J Lipid Res 51, 2863–2895.
Visser WF, van Roermund CW, Ijlst L, Waterham HR, Wanders RJ (2007). Metabolite transport across the peroxisomal membrane. Biochem J 401, 365–375.
Williams CP, Stanley WA (2010). Peroxin 5: a cycling receptor for protein translocation into peroxisomes. Int J Biochem Cell Biol 42, 1771–1774.
Wood CS, Koepke JI, Teng H, Boucher KK, Katz S, Chang P, Terlecky LJ, Papanayotou I, Walton PA, Terlecky SR (2006). Hypocatalasemic fibroblasts accumulate hydrogen peroxide and display age-associated pathologies. Traffic 7, 97–107.
Yano T, Oku M, Akeyama N, Itoyama A, Yurimoto H, Kuge S, Fujiki Y, Sakai Y (2010). A novel fluorescent sensor protein for visualization of redox states in the cytoplasm and in peroxisomes. Mol Cell Biol 30, 3758–3766.